Reduced state sequence detection of partial response continuous phase modulation

A. Svensson, PhD

Indexing terms: Detection, Modulation, State machines, Viterbi decoding

Abstract: A reduced state sequence detector (RSSD) which combines decision feedback with Viterbi decoding is proposed for partial response continuous phase modulation (CPM). This detector can successfully be used for both binary and high-level partial response CPM schemes. This detector is analysed by means of minimum Euclidean distance and by simulations of the symbol error probability. It is shown that the phase states in the receiver trellis of the maximum likelihood detector for partial response CPM can be exchanged by decision feedback in the metric calculations. This can be achieved without sacrificing minimum Euclidean distance of the first error event or symbol error probability. This RSSD is most attractive for narrow-band CPM schemes and at most about 2 dB in increased energy efficiency as compared with MSK is possible. Further reductions in number of states is possible, especially for high-level CPM schemes, by reducing the number of correlative states. For the most frequently used CPM schemes this can be done with a very small degradation in error performance. In this class of schemes, a complexity reduction of at least a factor five to ten is possible.

1 Introduction

Digital continuous phase modulations (CPM) are attractive because of their power efficiency, spectral efficiency and constant amplitude [1, 2]. In this class of modulations, schemes exist that save both power and bandwidth as compared with binary minimum shift keying (MSK). The optimum maximum likelihood sequence detector (MLSD) for these schemes on an additive white Gaussian noise channel consists of a filter bank followed by a Viterbi detector (VD). The large number of states needed to describe the CPM signal, means that this MLSD becomes complex to implement [1]. This is further emphasized when the CPM scheme is combined with convolutional encoding [1–5]. Techniques to reduce the complexity of this optimum Viterbi detector by means of oversampled and reduced-state sequential detectors [2, 6] have been studied but the obtained complexity reduction is quite small. Decoders based on limited search algorithms have also been studied for CPM schemes [7, 8]. These algorithms do not intend to reduce the number of states in the trellis. Instead they try to decode the signal in an optimum manner by following only a limited number of branches in the trellis or phase tree. These algorithms have been shown to be quite successful in terms of reducing the decoding complexity and these decoders are used for comparison.

Eyuboğlu and Qureshi [9] describe a highly structured reduced state sequence estimator (RSSE) for intersymbol interference (ISI) channels. A reduced state subset trellis for the ISI channel is constructed using set partitioning principles. A conventional Viterbi algorithm (VA) is combined with decision feedback and used to search for the best candidate sequence in this reduced state trellis. These ideas are generalised and applied to trellis coded modulations (TCM) on ISI channels in Reference 10. Similar results for both uncoded and coded linear modulations on ISI channels were also presented by Duel-Hallen and Heegard [11] and Chevillat and Eleftheriou [12].

The ideas of reduced state sequence detection (RSSD)* combined with decision feedback are applied to partial response CPM. The memory in partial response CPM differs from the memory introduced by an ISI channel and the memory in TCM in that the CPM signal depends not only on the correlative coding but also on the accumulated previously transmitted data symbols through the so called phase state. A reduced number of modified phase states can be defined and used with Viterbi detection combined with decision feedback without significantly degrading error performance [13]. RSSD for full response CPM has thus proved to be very useful, especially for most of the modulation indices of practical interest where only two modified phase states are required in the RSSD.

These ideas of modified phase states are generalised to partial response CPM and correlative states are fused into superstates. Reduced state sequence detection of partial response CPM was also considered in Reference 6, where the number of correlative states is reduced by using a detector for a CPM scheme which is based on a shorter frequency pulse. This also reduces the number of correlators required to find the metrics. The difference in the proposed method is that both the number of correlative states and phase states are reduced. This leads to a significantly smaller number of states.

It may be misleading to call the proposed detector a reduced state detector†. Reduced state detection has been used for some time as a name to describe other techniques, such as truncation of trellis generator and the retention of a state variable other than the data symbols.

Paper 8134I (E7, E8), first received 19th February 1990 and in revised form 18th April 1991

The author is with Ericsson Radar Electronics AB, Microwave Communications Division, Mobile Telephone Systems Department, Bergfotsgatan 2, S-431 84 Mölndal, Sweden

* RSSD is actually equal to RSSE, but the word detection is used instead of estimation since a sequence of symbols is being detected

† J.B. Anderson, private communications.

Reduced state detectors mostly have a degraded performance compared with the corresponding optimum detector. The technique proposed could also be referred to as trellis fusion, that is, fusion of states into substates,

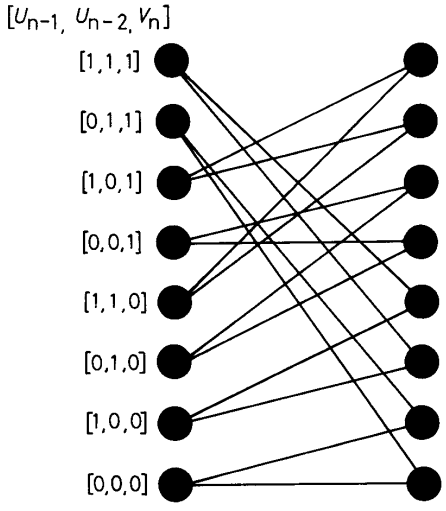

Fig. 1 *Section of ML trellis corresponding to binary CPM signal $L = 3$; $h = 1/2$*

in such a way that when the identity of states in the subsets is lost, the remaining code structure still has the same free distance. Some of the code structures, used by the detectors studied, have the same free distance as the code structure of the transmitted CPM signal, but this is obtained with a smaller number of states. The name reduced state detection has been chosen since the proposed detector has a reduced number of states compared with the trellis that describes the transmitted CPM signal. The decoder states of the reduced state detector proposed are not always obtained by trellis fusion, as will be explained in more detail.

The state description of partial response CPM is first reviewed. It is assumed that the reader is familiar with the definition of CPM. Only the definitions that are important in this method are considered. Modified states and superstates are introduced for CPM and the way in which the VA can be combined with decision feedback and used to find the most likely allowed path in the reduced state (RS) trellis is described. The decoding performance is analysed by means of minimum Euclidean distance and computer simulations on the error probability. Numerical results are given for binary and quaternary 3RC.

2 State description of CPM

A CPM scheme has been defined in great detail [1, 14]. The physical tilted phase introduced by Rimoldi [14] will be used. Only rational modulation indices of the form $h = K/P$, where K and P are relatively prime positive integers, are considered. The physical tilted phase is, in any symbol interval $nT \leqslant t < (n+1)T$, given by

$$\bar{\psi}(\tau + nT, \boldsymbol{U}) = R_{2\pi}\left[2\pi h R_P\left(\sum_{i=-\infty}^{n-L} U_i\right) + 4\pi h \sum_{i=0}^{L-1} U_{n-i} f(\tau + iT) + W(\tau)\right] \quad (1)$$

where $0 \leqslant \tau < T$, $\boldsymbol{U} = (\ldots, U_{n-1}, U_n)$ is the sequence of data symbols, L is the length in symbol intervals of the frequency pulse function, $f(t)$ is the phase response, $R_{2\pi}[\cdot]$ is the modulo 2π operator and $R_P(\cdot)$ is the modulo P operator for integers. The data symbols are M-ary, i.e. $U_i \in \{0, 1, \ldots, M-1\}$. The last term $W(\tau)$ is a data independent term [14].

From eqn. 1 [14] it is clear that the state at time $t = nT$ of the CPM signal is defined by

$$\boldsymbol{\sigma}_n = [U_{n-1}, \ldots, U_{n-L+1}, V_n] \quad (2)$$

where

$$V_n = R_P\left(\sum_{i=-\infty}^{n-L} U_i\right) \quad (3)$$

is the phase state. The total number of states is $S_{ML} = M^{L-1}P$, where P is the total number of phase states and M^{L-1} is the total number of correlative states [1]. This state is referred to as an ML state and the corresponding trellis is referred to as an ML trellis. An example of one section of an ML trellis is given in Fig. 1 when $M = 2$, $L = 3$ and $h = 1/2$.

3 RSSD with decision feedback for CPM

3.1 Modified state for CPM

The primary idea behind RSSD is to construct a trellis with a reduced number of states compared with the ML trellis and to use this trellis in the VD. This should preferably be achieved without sacrificing error performance. A VD is proposed that uses an RS trellis based on the modified state defined by

$$\boldsymbol{\sigma}'_n = [R_{M'_1}(U_{n-1}), \ldots, R_{M'_{L-1}}(U_{n-L+1}), V'_n(P', L')] \quad (4)$$

where

$$V'_n(P', L') = R_{P'}\left(\sum_{i=-\infty}^{n-L'} U_i\right) \quad (5)$$

$1 \leqslant M'_i \leqslant M$ for $1 \leqslant i \leqslant L-1$, $1 \leqslant L' \leqslant L$ and $1 \leqslant P' \leqslant P$. In general, M'_i can take any value between one and M, but since M is a power of two, M'_i is restricted to be a power of two, i.e. $\log_2 M'_i$ is an integer for all i in the interval $1 \leqslant i \leqslant L-1$. This does not seem to be a serious restriction, and it is not believed that RS trellises with significantly better performance are obtained for other values of M'_i. The first $L-1$ terms in eqn. 4, which directly depend on the last $L-1$ data symbols, will be referred to as the correlative superstate, since the superstate is constructed by fusing several ML correlative states in eqn. 2 into a superstate. This may also be referred to as correlative state fusion. Since each component in the modified state vector is based on a modulo operation, a component can be disregarded by choosing the modulo one operation for that component. Whenever this is done, the corresponding component will be omitted in the vector instead of writing 0 in that position. When $M'_i = M$ for $1 \leqslant i \leqslant L'' - 1$ and $M'_i = 1$ for $L'' \leqslant i \leqslant L-1$, where L'' is a positive integer less than L, the correlative superstate is a truncated correlative state. The total number of correlative superstates is $\prod_{i=1}^{L-1} M'_i$ and this is always a divisor of M^{L-1} when $\log_2 M'_i$ is an integer for all i.

The last component of the modified state in eqn. 4, i.e. $V'_n(P', L')$, is a modified phase state and can take P' different values [13]. Note that with $P' = P$, $V'_n(P, L')$ is also an ML phase state only differing from the ML phase state in eqn. 3 through the number of terms in the sum-

mation [1, 14]. This does not lead to any reduction in number of phase states. It simply leads to a renumbering of the ML states in eqn. 2. However, for $P' < P$ a reduction is obtained but this reduction is obtained differently depending on whether P' is a divisor of P or not [13]. The introduction of the complexity reduction concept is most easily visualised when P' is a divisor of P. The RS trellis obtained for this case is directly constructed from the ML trellis by state or trellis fusion and therefore deserve some attention. This case also has some interesting similarities with reduced complexity detectors [9–12]. This special case is first pursued and then it can easily be generalised to the case when P' is not a divisor of P. For both of these cases, the total number of modified states is given by

$$S_{RS} = P' \prod_{i=1}^{L-1} M_i' \tag{6}$$

3.2 P' is a divisor of P

3.2.1 Reduced state trellis: Whenever, P' is a divisor of P, P/P' and S_{ML}/S_{RS} are integers. The case $P' = 1$, which is shown to be an important case, belongs to this class. For this case

$$V_n'(P', L') = R_{P'}\left(R_P\left\{\sum_{i=-\infty}^{n-L'} U_i\right\}\right) = R_{P'}\{V_n'(P, L')\}$$

and the modified phase state is constructed by fusing ML phase states into phase superstates similarly to the correlative superstates above. This may also be referred to as phase state fusion. This in turn means that, the RS trellis is constructed by fusing S_{ML}/S_{RS} states in the ML trellis based on the phase state $V_n'(P, L')$ into one superstate and this is trellis fusion in the strict sense.

In this case, the information contained in the state vector σ_n can be decomposed into two superstate vectors such that

$$\sigma_n = \sigma_n' \times \sigma_n'' \tag{7}$$

The two vectors together uniquely define the state of the CPM signal. In the ML trellis there are M branches leaving each ML state, each corresponding to a different data symbol. For a partial response scheme, none of these are parallel transitions since the current data symbol is included in the next state. The state fusion in the RS trellis, means that there are MS_{ML}/S_{RS} branches leaving each RS state. These are collected in M clusters, each with S_{ML}/S_{RS} parallel transitions corresponding to the same data symbol but different CPM signals. When S_{RS} is small, e.g. $S_{RS} < M$, some of these clusters leave and enter the same pair of states, i.e. they are also parallel transitions. This is similar to e.g. 4-ary CPFSK with $h = 1/2$ that has two states but four branches leaving each state. The difference is that each transition is now a cluster of transitions. This is also similar to the RS trellis for ISI channels or some TCMs or combinations thereof [9–12].

For binary schemes M_i' for $1 \leqslant i \leqslant L-1$ can be one or two. The main interest for binary schemes turns out to be $M_i' = 2$ for $1 \leqslant i \leqslant L-1$ combined with $P' = 1$ or $P' = 2$. i.e. correlative states combined with one or two phase superstates. Also of interest is $L' < L$, $M_i' = 2$ for $1 \leqslant i \leqslant L'-1$ and $M_i' = 1$ for $L' \leqslant i \leqslant L-1$ combined with $P' = 1$, $P' = 2$ or $P' = P$, i.e. a truncated correlative state with one, two or P phase superstates. For the moment P must be an even integer when $P' = 2$ so that $P/2$ is an integer, but this assumption shall be removed. The choice $P' = P$ is similar to the ideas used in Reference 6 except that an ML metric combined with decision feedback† is used instead of a mismatched metric [6]. In Reference 6 the mismatched metric is also combined with a change in sampling time.

A RS trellis for $P' = 1$, $M_1' = 2$, $M_2' = 2$ and $M_i' = 1$ for $i > 2$ is shown in Fig. 2*a*. The trellis fusion that takes

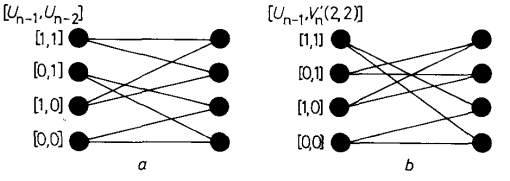

Fig. 2 *Two examples of section of RS trellis with four states for binary modulations*

place is described in more detail in the Appendix and Table 3. This trellis has no phase states, since all ML states with identical correlative states but different phase states are fused into one superstate. The information contained in the phase state is not used by the decoder when this trellis is employed. This trellis can be used with any binary CPM scheme with $L \geqslant 3$. When this trellis is used with binary 3RC, each line showing a transition corresponds to P parallel transitions each carrying a different signal corresponding to the same data symbol but differing through a constant phase shift. If the ML trellis is as given in Fig. 1, the two ML states [0, 0, 0] and [0, 0, 1] are fused into the superstate [0, 0]. This means that the transitions leaving these two states and entering the same two states correspond to a parallel transition leaving state [0, 0] and entering this same state in the RS trellis. In this example, all transitions shown in Fig. 2*a* must correspond to two parallel transitions.

When it is used with a scheme based on a frequency pulse of length $L > 3$, not only are phase states fused into one state but all ML correlative states having different symbols in the last $L-3$ positions but equal symbols in the first two positions are also fused. For binary 4RC with $h = 1/2$, the ML states [0, 0, 0, 0], [0, 0, 0, 1], [0, 0, 1, 0] and [0, 0, 1, 1] all fuse into the RS state [0, 0]. All transitions leaving these four ML states leave the same RS state. The number of parallel transitions is four and in general it is $2^{L-3}P$. The corresponding signals not only differ through a constant phase but also directly through the data symbols $U_{n-3}, \ldots, U_{n-L+1}$.

Another similar RS trellis with four states for binary 3RC is shown in Fig. 2*b*. This trellis corresponds to $P' = 2$, $L' = 2$ and $M_1' = 2$ and also has P parallel transitions, but these are not the same as in the trellis of Fig. 2*a*. This is clearly demonstrated in one example given in Table 4 in the Appendix where the transitions are shown. The signals on the parallel transitions do not differ through a constant phase when $h = 1/2$ but rather directly through the data symbol U_{n-2}. When this RS trellis is constructed from the trellis in Fig. 1, as is the case in Table 4, the two ML states [0, 0, 0] and [0, 1, 1] are fused into the superstate [0, 0], which is different from the RS trellis in Fig. 2*a*. The four transitions leaving the two ML states are now all leaving the same RS state leading to two parallel transitions in the RS trellis. The transitions of the two trellises in Fig. 2 are different,

† In the next subsection it becomes clear that this is also a mismatched metric after an error has occurred during the decoding.

compare Tables 3 and 4. It is shown that the error performance may be different for these two trellises when used with binary 3RC. These trellises do not depend on the modulation index of the scheme as is the case for the ML trellis. This is one of the ideas behind the trellis fusion technique proposed.

All possible paths through the RS trellis do not only describe all paths through the ML trellis, i.e. all CPM signals of the considered scheme, but also some other paths that are not described by the ML trellis. Each RS trellis section contains each possible CPM signal over one symbol interval just as is the case in the ML trellis. This is demonstrated for some examples in the Appendix. Since the ML states are fused into a smaller number of RS states, the identity of ML states are lost. The wrapping of transitions that appear because of the state fusion, lead to the fact that the transitions in the RS trellis may follow each other in a manner that is not possible in the ML trellis. From Fig. 2*a* and Table 3, the path described by the transitions a, j, l is a valid path in the RS trellis starting in RS state [0, 0] and ending in RS state [1, 1]. In Fig. 1 and Table 2, transition a goes from ML state [0, 0, 0] back to ML state [0, 0, 0]. It is then necessary to continue by transition a or b. This means that transition a may not be followed by transition j in the ML trellis. The path a, j, l in the RS trellis does not therefore describe a valid path in the ML trellis. The phase of all the signals described by the RS trellis can not be described as the phase of a CPM signal. The total number of signals described by the RS trellis is increased compared with the number of signals described by the ML trellis. This generally leads to a decreased minimum Euclidean distance in the RS trellis compared with the ML trellis. The RSSD has to overcome this penalty.

For high-level schemes there are many more possibilities for defining superstates since each M'_i can take $1 + \log_2 M$ different values when M'_i is restricted to be a power of two. One choice that is pursued is $M'_i = 2$ for some i values, which means that only information on whether one or several of the symbols in the ML correlative state are even or odd is used in the superstate. As an example one could use $\sigma'_n = [U_{n-1}, R_2(U_{n-2})]$ for M-ary schemes based on frequency pulses of length at least $L = 3$. The number of superstates for quaternary schemes is then eight compared with $4^{L-1}P$ for the ML decoder. This is a large reduction in number of states especially when P is large. This superstate can also be combined with two phase superstates leading to the superstate $\sigma'_n = [U_{n-1}, R_2(U_{n-2}), V'_n(2, L')]$. All these ideas have not been previously exploited for CPM schemes.

The vector σ''_n, which together with the superstate defines the ML state, is also a superstate but is not explicitly used by the RSSD. Using

$$U_{n-i} = R_{M'_i}(U_{n-i}) + \left\lfloor \frac{U_{n-i}}{M'_i} \right\rfloor M'_i$$

for all values on i and any $M'_i \leqslant M$ and

$$V'_n(P, L') = R_{P'}\left(\sum_{i=-\infty}^{n-L'} U_i\right) + \left\lfloor \frac{V'_n(P, L')}{P'} \right\rfloor P'$$

for all $P' \leqslant P$ such that P/P' is an integer, an expression for σ''_n can easily be obtained. $\lfloor \cdot \rfloor$ denotes the largest integer less than or equal to the argument. σ''_n is given by

$$\sigma''_n = \left[\left\lfloor \frac{U_{n-1}}{M'_1} \right\rfloor, \ldots, \left\lfloor \frac{U_{n-L+1}}{M'_{L-1}} \right\rfloor, \left\lfloor \frac{V'_n(P, L')}{P'} \right\rfloor\right] \quad (8)$$

The ML state is given by

$$\sigma'_n + \sigma''_n \text{ diag } (M'_1, \ldots, M'_{L-1}, P')$$

where diag $(\cdot, \ldots, \cdot)$ denotes a diagonal matrix. This is not exactly equal to the ML state σ_n as defined in eqn. 2 but is simply a renumbering of the states when $L' \neq L$.

3.2.2 Decision feedback: The optimum ML detector for CPM has been given in great detail [1]. All details not necessary are therefore omitted. The notation

$$\sigma_n : U'_n \rightarrow \sigma_{n+1} \quad (9)$$

is used to denote the transition from state σ_n to state σ_{n+1} that occurs because of the data symbol U'_n at time nT [12]. It is well known that the ML branch metric to be used by the VA for this transition is given by [1]

$$Z(\sigma_n : U'_n \rightarrow \sigma_{n+1}) = \int_{nT}^{(n+1)T} r(t)s(t, U'_n, \sigma_n)\, dt \quad (10)$$

where $r(t)$ is the received signal in additive white Gaussian noise and $s(t, U'_n, \sigma_n)$ is a CPM candidate signal corresponding to the considered branch in the ML trellis. This metric can be expressed in several different ways [1, 14].

In the VD using the ML trellis, the branch metric is computed for every possible branch in a trellis section. The VA then finds the most likely path through the states of the ML trellis. This can also be done in the RS trellis. Using the decomposition in eqn. 7, each transition in the ML trellis can be rewritten

$$\sigma'_n \times \sigma''_n : U'_n \rightarrow \sigma'_{n+1} \times \sigma''_{n+1}$$

Since the RS trellis is based on σ'_n, a transition in the RS trellis is given by

$$\sigma'_n : U'_n \rightarrow \sigma'_{n+1} \quad (11)$$

and this means that each possible value of σ''_n leads to a parallel transition. One of the parallel transitions corresponding to each data symbol must first be selected e.g. based on a hard decision on the corresponding branch metrics. When this hard decision is performed, there are no parallel transitions between states σ'_n and σ'_{n+1} except for those corresponding to different data symbols. The VA can be used in the traditional way to find the most likely path through the states of the RS trellis. This generally leads to a significantly degraded error performance. The reason for this is that the identity of the ML states is lost in the RS trellis and this decoding procedure may therefore select a path through the RS trellis that is not a valid path in the ML trellis. In general the free distance in the RS trellis is smaller than the free distance in the ML trellis. This may be overcome, during the decoding in the RS trellis, by disregarding all paths in the RS trellis that are not valid paths in the ML trellis.

The key idea to improve the performance is to select only those transitions in the nth trellis section that correspond to a valid path in the ML trellis when connected with the survivor path from the previous step of the VA in the RS trellis. This can be performed without comparing branch metrics. Only those branch metrics required by the VA have to be computed. This will guarantee that only CPM signals are compared when the VA selects the most likely transmitted path, although the decoding is performed in the RS trellis.

Assume that, at time nT, σ''_n is known at each superstate σ'_n. This means that the full state description σ_n is known at each superstate. Only one of the parallel tran-

sitions $\sigma'_n : U'_n \rightarrow \sigma'_{n+1}$ is also a transition $\sigma'_n \times \sigma''_n : U'_n \rightarrow \sigma'_{n+1} \times \sigma''_{n+1}$ in the ML trellis for that particular σ''_n. The branch metric $Z(\sigma'_n : U'_n \rightarrow \sigma'_{n+1})$ for this transition is given by the righthand side of eqn. 10 simply by exchanging σ_n with $\sigma'_n \times \sigma''_n$. The superstate σ''_n at each superstate σ'_n is in practice unknown and have to be estimated. From eqn. 8 it is found that σ''_n is defined based solely on data symbols preceeding the current trellis section and therefore can be estimated by

$$\hat{\sigma}''_n(\sigma'_n) = \left[\left[\frac{\tilde{U}_{n-1}}{M'_1} \right], \ldots, \left[\frac{\tilde{U}_{n-L+1}}{M'_{L-1}} \right], \left[\frac{R_P\left(\sum_{i=-\infty}^{n-L'} \tilde{U}_i \right)}{P'} \right] \right] \tag{12}$$

where $\tilde{U}_i$ for $i < n$ are the survivor symbols to state σ'_n. This explains the notation $\hat{\sigma}''_n(\sigma'_n)$. This is simply a form of decision feedback at each superstate. With this decision feedback, the RS trellis can be viewed as consisting of S_{RS} ML states σ_n and the succeeding ML states σ_{n+1} reduced to S_{RS} superstates through the superstate definition. These states are selected in a time varying manner based on decision feedback and the superstate definition. This time varying trellis has no parallel transitions except when the ML trellis has parallel transitions. The decision feedback can also be interpreted as selecting states and the corresponding signals in the ML trellis instead of selecting one out of several parallel transitions in the fused ML trellis. This interpretation is useful when generalised to any value of P'.

The branch metric $Z(\sigma'_n : U'_n \rightarrow \sigma'_{n+1})$ used by RSSD in each trellis section is given by the righthand side of eqn. 10 simply by exchanging σ_n with $\sigma'_n \times \hat{\sigma}''_n(\sigma'_n)$. When this RSSD algorithm with decision feedback is to be implemented it is more straightforward to keep at each state σ'_n an estimate of the ML state σ_n according to eqn. 7. This estimate, denoted $\hat{\sigma}_n(\sigma'_n)$, is (eqn. 2) given by

$$\hat{\sigma}_n(\sigma'_n) = \left[\tilde{U}_{n-1}, \ldots, \tilde{U}_{n-L+1}, R_P\left(\sum_{i=-\infty}^{n-L} \tilde{U}_i \right) \right] \tag{13}$$

With this ML state estimate, the branch metric is given by

$$Z(\sigma'_n : U'_n \rightarrow \sigma'_{n+1}) = \int_{nT}^{(n+1)T} r(t) s(t, U'_n, \hat{\sigma}_n(\sigma'_n))\, dt \tag{14}$$

This has been used in the simulations which will be presented. These metrics are generated by the same filter bank used by the MLSD. As long as the transmitted sequence is a survivor, a correlation is performed with the transmitted signal, but whenever the transmitted sequence is lost, the metric is a mismatched metric [6]. In the Appendix an example illustrating the update of the survivor path for one of the RS states in the RS trellis is pursued. The interested reader is referred to this example for further explanation of the decoding algorithm.

3.3 Any value of P'

The restriction that P' is a divisor of P is removed. Whenever, P' is not a divisor of P

$$V'_n(P', L') \neq R_{P'}\left(R_P\left\{ \sum_{i=-\infty}^{n-L'} U_i \right\} \right) = R_{P'}\{V'_n(P, L')\}$$

and the RS trellis can not be constructed by fusing states in the ML trellis into superstates. The superstates could, of course, be defined as the righthand side of the above equation and for this choice the RS trellis is for any value of P' constructed by fusing ML states into superstates. With this superstate definition the transitions caused by a given data symbol from a given superstate are not always entering the same superstate at the next time unit, when P' is not a divisor of P. The transitions from each superstate are not collected in M clusters, where each cluster contains parallel transitions corresponding to the same data symbol, as is the case when P' is a divisor of P. Each superstate does not contain the same number of ML states. This trellis sometimes has early mergers because of this non-clustering effect. The most disadvantageous effect of this superstate definition is that the transitions in each trellis section of the RS trellis, when used with RSSD, will depend on the decision feedback such that the RS trellis becomes time varying. The modified state as defined in eqn. 4 has been found to be the most promising state definition for the RS trellis.

Fig. 3 shows an example of an ML trellis for $L = 2$ and $P = 3$ and the corresponding RS trellis based on the

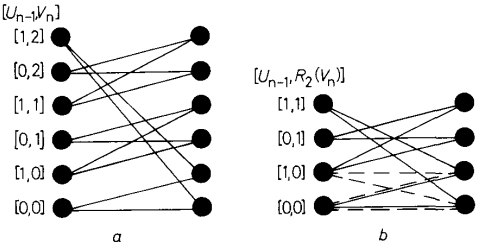

Fig. 3 *Section of ML trellis*

The transitions from states [0, 2] and [1, 2] in the ML trellis are shown dashed in the RS trellis

a $M = 2; L = 2; P = 3$

b RS trellis based on superstate $[U_{n-1}, R_2(V_n)]$

superstate $[U_{n-1}, R_2(V_n)]$ $(R_2(V_n) = R_2(V'_n(P, L)))$. These could be the trellises for binary 2RC with $h = 2/3$. The transitions from the ML states [0, 2] and [1, 2] are dashed in the RS trellis. For this RS trellis there are four transitions leaving the superstate [1, 0]. These are not two clusters of parallel transitions caused by data symbol zero and one, as is the case for superstate [0, 0] and also for any superstate state when P' is a divisor of P (Fig. 2). The solid and dashed transitions will be chosen in a time varying manner because of the decision feedback. The RS trellis in this example is not a binary time invariant trellis. This example reveals that the RS trellis based on the superstate $[R_2(V_n)]$ is also time varying, note the different data symbols on the parallel transitions, as is the RS trellis based on the superstate $[R_2(V'_n(2, 1))]$.

The decision feedback in RSSD was interpreted as selecting S_{RS} ML states including the signals on the transitions leaving these states and their succeeding states reduced through the modified state definition in a time varying manner. This is done in such a way that the underlying RS trellis, which is used by the VA, is time invariant. With this interpretation it is immediately evident that the modified states used by RSSD do not need to have any direct relationship with the ML states, because the ML state estimate $\hat{\sigma}_n(\sigma'_n)$ according to eqn. 13 keeps track of the CPM candidate signals to be used in the next trellis section. This is also clear from the metric increment given in eqn. 14. The only requirement is that there are M transitions leaving and entering each modifed state in the RS trellis such that all M-ary symbols are represented.

Any trellis with M transitions leaving each state is adequate with RSSD. Returning to the case when P' is not a divisor of P, it is observed that with $P = P'$ in eqn.

3, eqn. 2 represents the ML state of an M-ary CPM signal with P' ML phase states. This CPM signal has a modulation index equal to $h' = K'/P'$ where K' and P' are relatively prime positive integers. This trellis has M transitions leaving each state and is an adequate trellis for RSSD. The modified state, according to eqn. 4, is now a superstate to the ML state for h'. The corresponding RS trellis is obtained by fusing states in the ML trellis for the CPM signal with modulation index h' (and P' phase states) into superstates. This is, done by fusing correlative ML states into correlative superstates only, since the reduction to P' modified phase states is first obtained by considering the modulation index h'. The discussion for P/P' equal to an integer now applies to the ML trellis for the CPM signal with modulation index h'. Returning to the example shown in Fig. 3, note that the RS trellis is an ML trellis when $P = 2$, and $h = 1/2$, if the dashed transitions are discarded. The RS trellis in Fig. 3*b* with transitions according to the solid lines only, is therefore an RS trellis based on the modified state according to eqn. 4 and may be used for binary 2RC with $h = 2/3$, and $h = 1/3$.

4 Error performance

With RSSD, the VD will make an error for the first time at time jT if up to that time, the correct path $\boldsymbol{U}$ accumulates a worse ML metric* than some incorrect path $\tilde{\boldsymbol{U}}$ that merges with $\boldsymbol{U}$ in the RS trellis at time jT. In the RS trellis, two paths merge if the modified states are equal. This means that a merger that occurs independently of the modulation index in the ML trellis [1] is always a merger also in the RS trellis, since the corresponding paths reach the same state. There are many mergers in the RS trellis that are not mergers in the ML trellis. These paths enter different ML states but the same RS state. Many of the mergers that occur only for certain modulation indices in the ML trellis are mergers in the RS trellis. The RS trellis has no mergers that occur only for certain modulation indices, since this trellis is independent of the modulation index. In a RSSD, once the correct path is discarded, there is a possibility of error propagation caused by the incorrect metrics that will be used for the next few trellis sections. This may increase the probability of again discarding the correct path over these few trellis sections.

The exact error probability of RSSD is difficult to analyse because of the decision feedback. The first error event probability of RSSD gains, significant insight of the performance of RSSD. The effects of decision feedback are studied by computer simulations. If $\boldsymbol{U}$ is the correct sequence and $\tilde{\boldsymbol{U}}$ is an incorrect sequence with $U_i = \tilde{U}_i$ for $i < k$ and the corresponding superstates σ'_i and $\tilde{\sigma}'_i$ are equal for $i = j > k$ but not equal for $k + 1 < i < j$ this is refered to as a first error event† at $t = jT$. The set of all such first error events, denoted E', depends on the superstate in use and, in general, contains the corresponding first error events in the ML trellis as a subset.

The squared normalised Euclidean distance of such a first error event in the ML trellis is discussed in great detail in Reference 1. At sufficiently large E_b/N_0, where E_b is the energy per transmitted bit and N_0 is the one-sided power spectral density of the white Gaussian noise, the error probability for a first error event can be approximated with

$$P_e \approx CQ\left(\left(\frac{d^2_{min} E_b}{N_0}\right)^{1/2}\right) \tag{15}$$

where, d^2_{min} is the minimum squared normalised Euclidean distance

$$d^2_{min} = \min_{\boldsymbol{U} - \tilde{\boldsymbol{U}} \in E'} d^2(\boldsymbol{U} - \tilde{\boldsymbol{U}}) \tag{16}$$

among the first error events at time jT and is only a function of the difference sequence [1] and C is an error coefficient equal to the average number of error events at distance d^2_{min}. This distance will be referred to simply as minimum distance. An upper bound d^2_B of the minimum distance can be found by using only first error events of short duration in the minimisation. This bound can always be made tight by considering error events of sufficiently long duration.

4.1 Numerical results on minimum distance

Fig. 4 shows the minimum distance of the first error event for binary 3RC with various RSSDs. It is possible

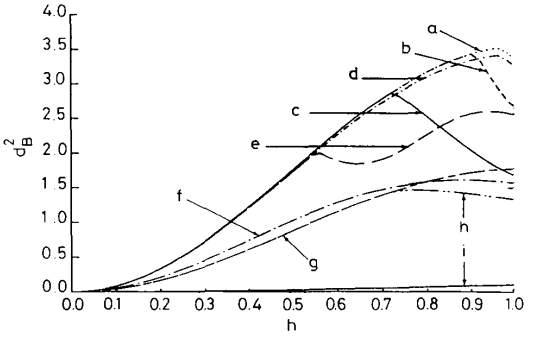

Fig. 4 *Upper bound on minimum distance for binary 3RC detected with RSSD*

All difference sequences which are nonzero over at most three symbols are considered in the upper bound
P is the number of phase states in the ML trellis.
a $[U_{n-1}, U_{n-2}, V'_n] = [U_{n-1}, U_{n-2}, V'_n(P, 3)]$
b $[U_{n-1}, U_{n-2}, V'_n(2, 3)]$
c $[U_{n-1}, U_{n-2}]$
d $[U_{n-1}, V'_n(P, 2)]$
e $[U_{n-1}, V'_n(2, 2)]$
f $[U_{n-1}]$
g $[V'_n(P, 1)]$
h $[V'_n(2, 1)]$
i no states

to use the superstate $[U_{n-1}, U_{n-2}]$ for all modulation indices less than 0.72 without any degradation in minimum distance. For these modulation indices the error event $\boldsymbol{U} - \tilde{\boldsymbol{U}} = \ldots, 0, 1, -1, 0, \ldots$ of length $4T$ is the minimum distance event. This error event is also the minimum distance event for the MLSD for all modulation indices less than 0.96. For larger modulation indices the error event $\boldsymbol{U} - \tilde{\boldsymbol{U}} = \ldots, 0, 1, 0, 0, \ldots$ of length $3T$ dominates the error performance of the RSSD and a degradation occurs†. By introducing the phase superstate $V'_n(2, 3)$, which is simply an ML phase state when $h = 0.5$, this is not any longer an error event and the minimum distance is at maximum for $h \leqslant 0.9$.

* The metric in eqn. 14 used by RSSD is an ML metric as long as no errors have occurred.

† This implies that the superstates are equal for all $i \leqslant k$ and that $U_k \neq \tilde{U}_k$.

† The sign reversed difference sequence, that corresponds to exchanging $\boldsymbol{U}$ and $\tilde{\boldsymbol{U}}$, always leads to the same distance as the difference sequence itself. Only the difference sequences with positive first non-zero component will be given.

When $R_{M_2'} = 1$ and therefore U_{n-2} is disregarded in the superstate, a significant degradation occurs when all phase states are in one phase superstate. The reason is that $U - \tilde{U} = \ldots, 0, 1, 0, \ldots$ now leads to a merger after $2T$. This merger is avoided by using the phase superstate $V_n'(2, 2)$ and the minimum distance is very close to maximum for $h \leqslant 0.54$. The merger is not avoided by using $V_n'(2, 3)$, because the last two symbols are not included in the phase superstate. The phase superstate $V_n'(2, 2)$ includes all previous symbols except the most recent. This improves the performance. It is therefore important to choose the correct phase superstate. It is worth noting that $[U_{n-1}, V_n'(2, 2)]$ is an ML state for, e.g. binary 2RC with modulation index $h = 0.5$. This trellis was also used with 3RC [6] but only for $h = 0.5$ and with correlators based on 2RC in the detector. Here, it is used for all modulation indices and with practically optimum performance for $h \leqslant 0.54$. This phase superstate is not enough to obtain a near optimum performance for larger modulation indices, where the event $U - \tilde{U} = \ldots, 0, 1, 1, 0, \ldots$ leads to a $3T$ merger. This merger is avoided with the phase superstate $V_n'(3, 2)$, i.e. by using three phase superstates. This leads to the same minimum distance as by using $V_n'(P, 2)$.

Similar arguments can be found for the case of using only phase superstates. This leads to a significantly reduced minimum distance. The conclusion is that for binary 3RC, an optimum minimum distance is reached with four states for most modulation indices of practical interest. For the larger modulation indices, a performance degradation will occur and the best RS trellis based on four superstates varies with modulation index. The two competing trellises are shown in Fig. 2. Fig. 2*b* shows the best trellis with four states for $h > 0.73$. The trellis in Fig. 2*a* obtains the minimum distance of the ML trellis for $h \leqslant 0.73$.

Minimum distance for quaternary 3RC with various RSSDs are shown in Fig. 5. For this scheme, the minimum distance for the ML detector is obtained for the error events $U - \tilde{U}$ equal to $\ldots, 0, 1, -2, 1, 0, \ldots, \ldots, 0, 1, -1, 0, \ldots, \ldots, 0, 3, -3, 0, \ldots$ and $\ldots, 0, 2, -2, 0, \ldots$ in the modulation index intervals (0, 0.55], [0.56, 0.59], [0.60, 0.73] and [0.74, 1.0], respectively. These error events are of lengths $5T$, $4T$, $4T$ and $4T$, respectively.

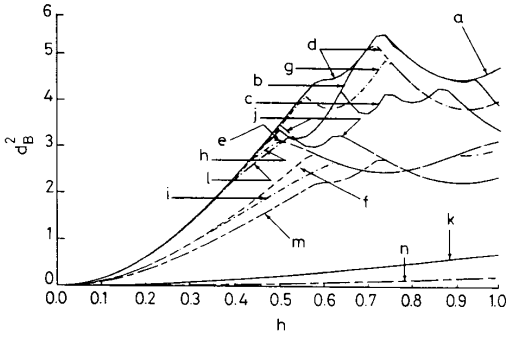

Fig. 5 *Upper bound on minimum distance for quaternary 3RC detected with RSSD*

All difference sequences which are nonzero over at most three symbols are considered in the upper bound
P is the number of phase states in the ML trellis
a $[U_{n-1}, U_{n-2}, V_n]$
b $[U_{n-1}, U_{n-2}, V_n'(2, 3)]$
c $[U_{n-1}, U_{n-2}]$
d $[U_{n-1}, R_2(U_{n-2}), V_n'(P, 2)]$
e $[U_{n-1}, R_2(U_{n-2}), V_n'(2, 2)]$
f $[U_{n-1}, R_2(U_{n-2})]$
g $[U_{n-1}, V_n'(P, 2)]$
h $[U_{n-1}, V_n'(2, 2)]$
i $[U_{n-1}]$
j $[R_2(U_{n-1}), R_2(U_{n-2}), V_n'(P, 1)]$
k $[R_2(U_{n-1}), R_2(U_{n-2}), V_n'(2, 1)]$, $[R_2(U_{n-1}), R_2(U_{n-2})]$, $[R_2(U_{n-1}), V_n'(2, 1)]$, $[R_2(U_{n-1})]$, $[V_n'(2, 1)]$
l $[R_2(U_{n-1}), V_n'(P, 1)]$
m $[V_n'(P, 1)]$
n no states

For RSSD, an optimum minimum distance is obtained with $[U_{n-1}, U_{n-2}]$ for $h \leqslant 0.44$. This always leads to 16 states. For $h > 0.44$, the difference sequences $(U - \tilde{U})$ equal to $\ldots, 0, 3, -1, 0, \ldots, \ldots, 0, 2, 0, \ldots, \ldots, 0, 3, 0, \ldots, \ldots, 0, 2, -1, 0, \ldots$ and $\ldots, 0, 1, 0, \ldots$, of lengths $4T$, $3T$, $3T$, $4T$ and $3T$, respectively, degrade the performance. The last three of these mergers are avoided by using the state $[U_{n-1}, U_{n-2}, V_n'(2, 3)]$. This improves the performance for some h-values at the expense of 32 states. For $h \leqslant 0.44$, a maximum distance is also obtained with the modified state $[U_{n-1}, R_2(U_{n-2}), V_n'(2, 2)]$, which also leads to 16 states. The difference sequences $\ldots, 0, 3, -1, 0, \ldots$ (only around $h = 0.46$) and $\ldots, 0, 2, 0, \ldots$ lead to $3T$ and $2T$ mergers, respectively, that significantly degrade the performance when $h > 0.44$. These mergers are avoided with the modified state $[U_{n-1}, R_2(U_{n-2}), V_n'(P, 2)]$. The distance is now at maximum for $h \leqslant 0.7$, but at the expense of $8P$ states. For larger modulation indices the performance is still degraded, but now because of a $3T$ merger for the difference sequence $\ldots, 0, 2, -2, 0, \ldots$. The modified state $[U_{n-1}, R_2(U_{n-2})]$ leads to a degradation for all modulation indices. For $h \leqslant 0.5$ a maximum distance can also be obtained with the modified state $[R_2(U_{n-1}), R_2(U_{n-2}), V_n'(P, 1)]$ with $4P$ states in total and $4P$ is smaller than 16 when $h = 1/3$ and $h = 1/2$. With this state, the difference sequences $\ldots, 0, 2, 0, -2, 0, \ldots$ and $\ldots, 0, 2, -2, 0, \ldots$ leads to $3T$ and $2T$ mergers, respectively. These mergers significantly degrade the performance when $h > 0.5$. Note that P phase states must be used with this modified state or the performance is drastically degraded.

A distance that is less than 0.1 dB from maximum, and therefore optimum from a practical point of view, is obtained when the $4T$ merger caused by the difference sequence $\ldots, 0, 1, -2, 1, 0, \ldots$ gives rise to the minimum distance. This happens for $h < 0.56$ when the modified state $[U_{n-1}, V_n'(P, 2)]$ is used. The number of states is again $4P$. For $h > 0.56$ the $3T$ mergers by the difference sequences $\ldots, 0, 3, -3, 0, \ldots$ and $\ldots, 0, 2, -2, 0, \ldots$, degrade the performance, but this degradation is less than 0.8 dB in minimum distance. For $h \leqslant 0.42$ this practically optimum performance from a distance point of view is also obtained with the modified state $[U_{n-1}, V_n'(2, 2)]$. The number of states is eight and the difference sequences $\ldots, 0, 1, -3, 0, \ldots$ and $\ldots, 0, 2, 0, \ldots$ with mergers of length $3T$ and $2T$, respectively, significantly degrade the performance for larger modulation indices. The modified state $[R_2(U_{n-1}), V_n'(P, 1)]$ with $2P$ states also leads to this near optimum minimum distance for all $h \leqslant 0.38$. For this state the difference sequences $\ldots, 0, 1, -3, 2, 0, \ldots, \ldots, 0, 2, 0, -2, 0, \ldots$ and $\ldots, 0, 2, -2, 0, \ldots$ with mergers of length $3T$, $3T$ and $2T$, respectively, significantly degrade the performance for larger modulation indices.

The modulation indices larger than say 0.5 are less interesting from a practical point of view. For these it is also clear that the difference in performance for the different RSSDs is generally much larger. More states are generally needed to obtain just a small degradation in minimum distance. All these comparisons can easily be done in Fig. 5 but are not commented on. A comparison between binary and quaternary 3RC is of some interest.

With only two states in the RSSD, binary 3RC obtains the best performance for a given h. With four and P states, quaternary 3RC obtains the largest minimum distance except when $h \in [0.66, 0.8]$ and the number of states is four. For $h \in (0, 0.65]$ and $h \in [0.95, 1]$, quaternary 3RC is also better than binary 3RC with eight states in the RSSD and with 16 states quaternary 3RC is always best. The conclusion is that for modulation indices of practical interest, say less than 0.5, quaternary 3RC is better than binary 3RC, from a first error event point of view, when decoded with RSSD with the same number of states, except when the number of states is only two. There may be some specific modulation indices for which this is not true but it is certainly true for most modulation indices in the interval considered.

4.2 Simulated symbol error probability

The minimum distance results do not take error propagation caused by decision feedback into account. The symbol error probability for RSSD has therefore been simulated with decision feedback according to eqn. 14. The decision depth in the RSSD is 20 symbols for all simulations. This should be enough to obtain the performance as predicted by the minimum distance. All simulations were performed with 25000 transmitted symbols. Bit error probability for binary 3RC with $h = 1/4$ is shown in Fig. 6 for six different RSSDs and

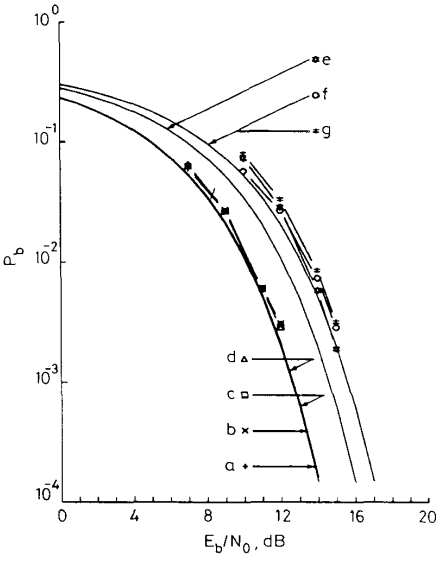

Fig. 6 *Simulated bit error probability for binary 3RC with $h = 1/4$ detected with RSSD*

The solid lines show the asymptotic performance as predicted by the minimum distance
a $[U_{n-1}, U_{n-2}, V_n]$
b $[U_{n-1}, U_{n-2}]$
c $[U_{n-1}, V'_n(P, 2)]$
d $[U_{n-1}, V'_n(2, 2)]$
e $[U_{n-1}]$
f $[V'_n(P, 1)]$
g $[V'_n(2, 1)]$

also for MLSD. The asymptotic performance as predicted by the minimum distance according to eqn. 15 with $C = 1$ is also shown by solid lines. Error propagation clearly does not degrade the performance except when the modified state is $[U_{n-1}]$. The excess degradation caused by error propagation is small for this case. The conclusion is that this scheme can be optimally detected with only four states in the detector compared with 16 for MLSD. With only two states, the degradation is about 2.5 dB at 10^{-3}. Simulations have shown that the error propagation is also negligible at $h = 1/2$.

The situation is different when $h = 4/5$ as shown in Fig. 7. The excess degradation caused by error propaga-

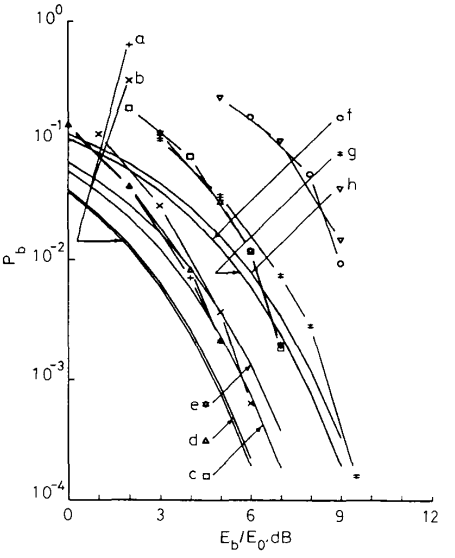

Fig. 7 *Simulated bit error probability for binary 3RC with $h = 4/5$ detected with RSSD*

The solid lines show the asymptotic performance as predicted by the minimum distance
a $[U_{n-1}, U_{n-2}, V_n]$
b $[U_{n-1}, U_{n-2}, V'_n(2, 3)]$
c $[U_{n-1}, U_{n-2}]$
d $[U_{n-1}, V'_n(P, 2)]$
e $[U_{n-1}, V'_n(2, 2)]$
f $[U_{n-1}]$
g $[V'_n(P, 1)]$
h $[V'_n(2, 1)]$

tion is negligible only for the modified state $[U_{n-1}, V'_n(P, 2)]$ but is small for $[U_{n-1}, U_{n-2}, V'_n(2, 3)]$. It is also quite small for $[V'_n(P, 1)]$ although the overall degradation is several decibels. From a practical point of view eight states are required to obtain a near optimum error performance as compared to 20 for MLSD. With four states the overall degradation is slightly more than 1 dB at 10^{-3}. It is several decibels with two states. The performance is better with four states than with five states.

The reason for the more severe error propagation when $h = 4/5$ as compared with $h = 1/4$ and $h = 1/2$ is found by studying the dominating error events. With $h = 1/4$, there is excess degradation caused by error propagation only with the modified state $[U_{n-1}]$. The dominating error event is obtained for the difference sequence $\boldsymbol{U} - \tilde{\boldsymbol{U}} = \ldots, 0, 1, 0, \ldots$ for this RSSD. It is obtained for $\boldsymbol{U} - \tilde{\boldsymbol{U}} = \ldots, 0, 1, -1, 0, \ldots$ for all other simulated RSSDs. However, $\boldsymbol{U} - \tilde{\boldsymbol{U}} = \ldots, 0, 1, -1, 0, \ldots$ is the dominating error event for the MLSD. The estimated ML states are therefore equal for both the correct and the erroneous sequence $L + 1$ symbols after the start of the error event. This means that no extra errors have to be made to return to the correct sequence after the dominating error has occurred. The error probability does not seem to increase because of the L incorrect metrics that are used during the error event.

With the difference sequence $\boldsymbol{U} - \tilde{\boldsymbol{U}} = \ldots, 0, 1, 0, \ldots,$ which is not an error event for MLSD, the situation is different. For these sequences the estimated ML states

are never equal after the error event, since the estimated ML phase states will always differ when the estimated ML correlative states are equal. The candidate signal used instead of the correct signal for the metric calculation will differ by a constant phase shift. At least one more error has to occur before the estimated ML state of the erroneous sequences equal to the ML state of the transmitted sequence. This error symbol must be -1 or the estimated ML states will not be equal until more errors have occurred. The second (and following) error(s) have to occur because of noise and therefore may not follow directly after the first error as for the ML error event. This means that incorrect metrics are used over a longer time interval leading to an increased sensitivity to error propagation.

For $h = 4/5$, the three RSSDs with small excess degradation because of error propagation have the ML error event as a dominating error event. All the other RSSDs have dominating error events corresponding to other sequences and therefore more errors caused by noise have to occur before the estimated ML state of the most likely signal is corrected to the ML state of the transmitted signal. The effect of using erroneous candidate signals in the metric calculation becomes more severe for larger h-values since the correct and incorrect signals differ more owing to the large frequency deviation. Error propagation is therefore negligible as long as the ML error events, with error symbols summing to zero, are the dominating error events. This means that RSSD is a promising technique for most practical binary CPM schemes.

Simulations of symbol error probability have also been performed for quaternary 3RC with $h = 1/3$. For this scheme, the complete error probability curves are not shown but Table 1 shows the E_b/N_0 value at which the symbol error probability equals 10^{-3}. For this scheme, the error propagation is negligible for most detectors. This agrees with the discussion. The error propagation is slightly larger for the detector on row seven, 10 and 11 in the Table. Simulations have verified that the error events for these detectors quite often start as a most likely error event but then change into a longer error event because of the erroneous metrics that are used. The most promising detector seems to be based on the state $[U_{n-1}, V'_n(2, 2)]$. The corresponding row in Table 1 is marked with an arrow. This detector has only eight states compared with 48 states for the optimum MLSD.

4.3 *Comparison with similar reduced complexity decoders*

The number of states required for this RSSD to obtain an optimum performance is compared with complexity measures for similar decoding algorithms [6–8]. RSSD outperforms the reduced state Viterbi detector [6] for most CPM schemes. The asymptotic performance of the detector [6] never reaches the asymptotic performance of MLSD when the number of states is reduced. A near optimum performance is obtained with half the number of states of MLSD. For some schemes with long frequency pulses, a rather good performance is also obtained with 1/4 of the number of MLSD states. The main advantage of RSSD is that the number of states is more or less independent of the number of phase states which is not the case for the Viterbi detector [6]. The advantage in complexity reduction of RSSD can thus be made very large by making the comparison at a proper modulation index. The Viterbi detector [6] can easily be modified to include decision feedback and the performance is then expected to be similar to RSSD as presented.

A limited trellis search algorithm for the decoding of CPM signals is proposed in Reference 7. Simulated symbol error probability is given for a variety of schemes [7]. The number of paths used by the trellis search algorithm and the number of states in RSSD when the performance is optimum or at least near optimum is compared. For the trellis search algorithm, four paths are required for both $h = 1/3$ and $h = 2/3$ with binary 3RC. Although there are no simulations for these modulation indices it is clear that four states are required for RSSD just as is the case when $h = 1/4$. The trellis search algorithm decodes quaternary 3RC with $h = 1/3$ with seven paths. RSSD needs eight states to obtain the same performance. Also for the other binary and quaternary schemes studied [7] it is concluded, based on distance calculations, that the number of states required by RSSD to obtain near optimum performance is approximately equal to the number of paths required by the trellis search algorithm. These decoders are thus very similar in terms of the number of paths and states required. RSSD is somewhat simpler to implement, since the trellis search algorithm involves a sorting among the extended paths at each trellis section and sorting is complex to implement.

A limited phase tree search algorithm for the decoding of CPM signals was proposed in Reference 8. It can be noted that the limited trellis search algorithm proposed in Reference 7 can also be employed in the phase tree. These two search algorithms are therefore quite similar. The rules for selecting the surviving path are different. The sorting done in the algorithm is replaced by a predetermined processing order which leads to a simpler detector. The phase tree search algorithm is only studied for binary schemes with rectangular pulses, but for these the complexity is reduced by a factor of P when $h = 1/P$ and by a factor of $P/2$ or $P/3$ when $h = K/P$ with $K > 1$.

Table 1: Simulated symbol error probability and corresponding asymptotic performance

State definition	Number of states	E_b/N_0 (dB) at which $Q((d^2_{min} E_b/N_0)^{1/2}) = 10^{-3}$	$P_s = 10^{-3}$	
$[U_{n-1}, U_{n-2}, V_n]$	48	7.57	8.6	
$[U_{n-1}, U_{n-2}, V'_n(2, 3)]$	32	7.57	8.6	
$[U_{n-1}, R_2(U_{n-2}), V'_n(P, 2)]$	24	7.57	8.6	
$[U_{n-1}, U_{n-2}]$	16	7.57	8.6	
$[U_{n-1}, R_2(U_{n-2}), V'_n(2, 2)]$	16	7.57	8.6	
$[U_{n-1}, V'_n(P, 2)]$	12	7.64	8.8	
$[R_2(U_{n-1}), R_2(U_{n-2}), V'_n(P, 1)]$	12	7.57	9.5	
$[U_{n-1}, V'_n(2, 2)]$	8	7.64	8.8	⇐
$[U_{n-1}, R_2(U_{n-2})]$	8	9.36	10.4	
$[R_2(U_{n-1}), V'_n(P, 1)]$	6	7.64	9.8	
$[U_{n-1}]$	4	9.40	11.2	

RSSD and the phase tree search algorithm have very similar complexity. For modulation indices $1/P$ the phase states are not required by RSSD and thus the complexity reduction is also P. With RSSD this is true for all modulation indices less than 0.7 for binary 3RC and therefore RSSD may be somewhat simpler for modulation indices between 0.5 and 0.7.

5 Discussion and conclusions

Reduced state sequence detection (RSSD) combined with decision feedback has been proposed for the decoding of CPM schemes. The performance is analysed by means of minimum Euclidean distance for the first error event and simulated symbol error probability. The distance results show that, for most modulation indices of practical interest, an RSSD based on only correlative states can be used without degrading the minimum distance. This leads to a complexity reduction equal to the number of phase states in the ML trellis. This is a significant number especially for many bandwidth efficient high-level schemes. Further reductions for nonbinary schemes are sometimes possible with only small degradations in minimum distance. Simulations of the symbol error probability verify that this performance is also obtained when decision feedback is employed. Another advantage of RSSD is that the number of states can be made independent of the modulation index. Any modulation index can therefore be chosen when selecting the modulation without bothering about decoding complexity. Thus, with RSSD more CPM schemes become practically implementable.

From an energy-bandwidth tradeoff [1] viewpoint RSSD is very attractive for the bandwidth saving, compared with MSK, CPM schemes. At most about 2 dB increase in energy efficiency, compared with MSK, can be achieved with RSSD with a significantly reduced number of decoder states. For most of these schemes with an alphabet of at least four, the modulation index is smaller than 1/2 and, especially for schemes with a narrow bandwidth, the modulation index is significantly smaller than 1/2. In this class of schemes a complexity reduction of a factor between P and $2P$, where P is the number of phase states in the MLSD, is possible, still maintaining an error performance equal to the ML performance. For many schemes of practical interest this means a complexity reduction of at least a factor of five to ten. These numbers on complexity reduction is similar to the numbers reported for the limited trellis and tree search algorithms [7, 8].

For CPM schemes with larger energy savings and with bandwidth at least equal to the MSK bandwidth, RSSD is less attractive. The reason for this is the larger value on the modulation index, leading to larger phase variations over each symbol interval. This makes it more difficult to reduce the number of states and preserve the performance. Small savings in complexity is possible, but these savings are comparable with the savings reported in References 6–8.

A computationally efficient decoding algorithm for CPM has been proposed. It is, outside the scope of this paper to find the optimum decoding algorithm from a computational efficiency point of view. More work needs to be done on this topic, but it is conjectured that the reductions in complexity reported is about the best possible with preserved performance equal to the ML performance, at least for the modulation indices used most frequently in practice. For the RSSDs with some degradation it may be possible to slightly increase the performance. It does not appear possible to reach the ML performance or to come close to the ML performance for those RSSDs with several decibels degradation. The RSSDs for which this may be possible are characterised by a dominating error event that is equal to the dominating ML error event with the ending tail significantly chopped. Examples are RSSD based on the modified state $[U_{n-1}, V'_n(2, 2)]$ for M-ary 3RC or $[V'_n(2, 1)]$ for binary 3RC. Those two RSSDs have a dominating error event based on the difference sequence $\ldots, 0, 1, -1, 0, \ldots$ for small modulation indices and binary schemes*, but the corresponding error event is one and two symbol intervals shorter than the corresponding ML error event. This shortening appears only at the ending tail of the ML error event and this significantly reduces the minimum distance especially in the second case. It is hoped that the results will stimulate researchers to do more work on decoding algorithms for CPM that are optimum from a complexity point of view.

A mismatched metric has been combined with a delay in sampling time [6] such that the shortening appears equally in both tails of the dominating ML error event. This may lead to an increased performance especially when the ML error event is significantly shortened, since the middle part of the error event contributes more distance than the tails. If the error event is shortened to half of the ML error event length, the decrease in distance is smaller if one quarter in each tail is discarded compared with the last half of the error event as is the case for the RSSD. The question is whether the decrease in distance caused by the mismatched metric is smaller than the increase in distance caused by the sampling time. There is a small gain to be made at least when a mismatched metric [15] is used†. The degradation without delayed sampling time is significant. This concept does not change the RS trellis to be used, but rather means that a CPM scheme based on a shorter frequency pulse is used in the decision feedback and metric calculation of the RSSD.

RSSD becomes very interesting for convolutionally encoded CPM schemes, since these schemes typically use quite small modulation index with a high-level CPM scheme. Significant savings in decoder complexity are foreseen. The convolutionally encoded CPM schemes mostly have quite long dominating error events [4]. This makes it harder to reduce the number of states while maintaining the minimum distance, since early mergers due to the complexity reduction more easily appear for long error events. Another way to approach convolutionally encoded CPM schemes may be to find the optimum convolutional code combined with a given CPM scheme for a given RS trellis, i.e. to optimise the scheme conditioned on a RSSD with a given decoder complexity.

6 Acknowledgment

The author wishes to thank G. Lindell at the University of Lund (Sweden) for many stimulating discussions during the progress of this work and J. B. Anderson at Rensselaer Polytechnic Institute (USA), who suggested the name trellis fusion and gave constructive comments on the manuscript.

* The RSSD based on the first modified state has a dominating error event based on the difference sequence $\ldots, 0, 1, -2, 1, 0, \ldots$ for quaternary 3RC, but the same arguments can be applied to this event.

† The concept of using a reduced set of basis functions [15] is not combined with a delayed sampling time but this can easily be done and will lead to an improved performance when used with RSSD.

7 References

1 ANDERSON, J.B., AULIN, T., and SUNDBERG, C.-E.: 'Digital phase modulation' (Plenum Press, New Jersey, 1986)
2 MASENG, T.: 'Digitally phase modulated (DPM) signals', *IEEE Trans.*, 1985, **COM-33,** (9), pp. 911–918
3 LINDELL, G., and SUNDBERG, C.-E.: 'An upper bound on the bit error probability of combined convolutional coding and continuous phase modulation', *IEEE Trans.*, 1988, **IT-34,** (5), pp. 1263–1269
4 LINDELL, G., SUNDBERG, C.-E., and AULIN, T.: 'Minimum Euclidean distance for combinations of short rate 1/2 convolutional codes and CPFSK modulation', *IEEE Trans.*, 1988, **IT-30,** (3), pp. 509–519
5 RIMOLDI, B.: 'Design of coded CPFSK modulation systems for bandwidth and energy efficiency', *IEEE Trans.*, 1989, **COM-37,** (9), pp. 897–905
6 SVENSSON, A., SUNDBERG, C.-E., and AULIN, T.: 'A class of reduced-complexity Viterbi detectors for partial response continous phase modulation', *IEEE Trans.*, 1984, **COM-32,** (10), pp. 1079–1087
7 AULIN, T.: 'A new trellis decoding algorithm — analysis and applications'. Technical Report 2, Division of Informations Theory, Chalmers University of Technology, Göteborg, Sweden, 1985
8 SIMMONS, S.J., and WITTKE, P.H.: 'Low complexity decoders for constant envelope modulations', *IEEE Trans.*, 1983, **COM-31,** (12), pp. 1273–1280
9 EYUBOĞLU, M.V., and QURESHI, S.U.H.: 'Reduced-state sequence estimation with set partitioning and decision feedback', *IEEE Trans.*, 1988, **COM-36,** (1), pp. 13–20
10 EYUBOĞLU, M.V., and QURESHI, S.U.H.: 'Reduced-state sequence estimation for coded modulation on intersymbol interference channels', *IEEE J. Sel. Areas Commun.*, 1989, **SAC-7,** (6), pp. 989–995
11 DUEL-HALLEN, A., and HEEGARD, C.: 'Delayed decision-feedback sequence detection', *IEEE Trans.*, 1989, **COM-37,** (5), pp. 428–436
12 CHEVILLAT, P.R., and ELEFTHERIOU, E.: 'Decoding of trellis-encoded signals in the presence of intersymbol interference and noise', *IEEE Trans.*, 1989, **COM-37,** (7), pp. 669–676
13 SVENSSON, A.: 'Reduced state sequence detection of full response continuous phase modulation', *Electron. Lett.*, 1990, **26,** (10), pp. 652–654
14 RIMOLDI, B.E.: 'A decomposition approach to CPM', *IEEE Trans.*, 1988, **IT-34,** (2), pp. 260–270
15 HUBER, J., and LIU, W.: 'An alternate approach to reduced-complexity CPM-receivers', *IEEE J. Sel. Areas Commun.*, 1989, **SAC-7,** (9), pp. 1437–1449

8 Appendix

8.1 Examples of RS trellises

The way in which an RS trellis is obtained is demonstrated. This is achieved by following some examples. The ML trellis for a binary scheme based on a pulse with length $L = 3$ and with modulation index $h = 1/2$ is shown in Fig. 1. This scheme is used in these examples and the different transitions are given in Table 2.

Consider an RS trellis for the above scheme which is based on the superstate $[U_{n-1}, U_{n-2}]$, i.e. $P' = 1, M'_1 = 2$ and $M'_2 = 2$. This means that all ML states with equal ML correlative state but different phase states are fused into on RS state. This RS trellis is shown in Fig. 2*a* and is given in more detail in Table 3. This Table shows the ML states that are fused into each RS state and the parallel transitions between each pair of current and next states. The interested reader can easily construct similar RS trellises when the ML trellis has more than two phase states. The only difference is that more ML states are fused into one RS state and more parallel transitions are therefore obtained.

An example showing how to obtain the RS trellis when the ML correlative state is truncated, and the truncated correlative state symbol is included in the modified phase state, is given. The RS state is therefore identical to the ML state for a scheme with $L = 2$ and $h = 1/2$. This trellis corresponds to $P' = P = 2$, $L' = 2$ and $M'_1 = 2$. Such a RS trellis is shown in Fig. 2*b* when $L \geqslant 3$ and $h = 1/2$. Assume that the ML trellis is as given in Table 2. The RS state is now given by $[U_{n-1}, V'_n(2, 2)]$ and is given in detail in Table 4. The transitions between states are different from the transitions in Table 3. There are still two parallel transitions between each pair of states.

Table 2: Description of ML trellis

Current state $[U_{n-1}, U_{n-2}, V_n]$	Next state $[U_{n-1}, U_{n-2}, V_n]$	Transition
[0, 0, 0]	[0, 0, 0]	a
	[1, 0, 0]	b
[1, 0, 0]	[0, 1, 0]	c
	[1, 1, 0]	d
[0, 1, 0]	[0, 0, 1]	e
	[1, 0, 1]	f
[1, 1, 0]	[0, 1, 1]	g
	[1, 1, 1]	h
[0, 0, 1]	[0, 0, 1]	i
	[1, 0, 1]	j
[1, 0, 1]	[0, 1, 1]	k
	[1, 1, 1]	l
[0, 1, 1]	[0, 0, 0]	m
	[1, 0, 0]	n
[1, 1, 1]	[0, 1, 0]	o
	[1, 1, 0]	p

Table 3: Description of RS trellis based on RS state $[U_{n-1}, U_{n-2}]$

Current RS state $[U_{n-1}, U_{n-2}]$	Fused from ML states $[U_{n-1}, U_{n-2}, V_n]$	Next RS state $[U_{n-1}, U_{n-2}]$	Transitions between RS states
[0, 0]	[0, 0, 0], [0, 0, 1]	[0, 0]	a, i
		[1, 0]	b, j
[1, 0]	[1, 0, 0], [1, 0, 1]	[0, 1]	c, k
		[1, 1]	d, l
[0, 1]	[0, 1, 0], [0, 1, 1]	[0, 0]	e, m
		[1, 0]	f, n
[1, 1]	[1, 1, 0], [1, 1, 1]	[0, 1]	g, o
		[1, 1]	h, p

From these two binary examples it becomes obvious how to construct RS trellises for other CPM schemes and other RS state definitions. The situation becomes slightly more complex when $P \geqslant 4$ and P' still is two or at least less than P. A complete trellis for this case is not given because of the space limit, but Table 5 shows the fusion of some states when $L = 3$ and $h = 1/8$. The proposed technique becomes clear with these examples.

No examples of the fusion of ML states for high-level schemes are given. All the examples of ML state fusion given in Table 5 are also valid for high-level schemes. For high-level schemes a modulo M'_i operation on some of the correlative state symbols may also be included in the RS state definition. This means that more ML states are fused into one RS state. It is straight forward to find these RS trellises.

8.2 Decoding example

An example of the decoding algorithm is given. The only difference compared with the convention VD for CPM is the calculation of the metric for each state in the RS trellis. An example of this is performed for one RS state. The example is based on $M = 2$, $L = 3$ and $h = 1/2$ with an ML trellis as shown in Fig. 1 and in Table 2. The RS

Table 4: Description of RS trellis based on RS state $[U_{n-1}, V'_n(2, 2)]$

Current RS state $[U_{n-1}, V'_n(2, 2)]$	Fused from ML states $[U_{n-1}, U_{n-2}, V_n]$	Next RS state $[U_{n-1}, V'_n(2, 2)]$	Transitions between RS states
[0, 0]	[0, 0, 0], [0, 1, 1]	[0, 0] [1, 0]	a, m b, n
[1, 0]	[1, 0, 0], [1, 1, 1]	[0, 1] [1, 1]	c, o d, p
[0, 1]	[0, 1, 0], [0, 0, 1]	[0, 1] [1, 1]	e, i f, j
[1, 1]	[1, 1, 0], [1, 0, 1]	[0, 0] [1, 0]	g, k h, l

trellis is assumed to be the trellis given in Fig. 2*a* and in Table 3. It is demonstrated how the decoder finds the survivor to RS state [0, 0] and the new ML state estimate for the same RS state which is to be used during the decoding in the next trellis section. The four possible transitions into RS state [0, 0] are shown in Fig. 8. The

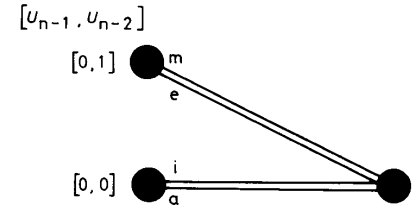

Fig. 8 *Available transitions during decoding at RS state [0, 0]*

transitions are denoted according to Table 2. Assume that transition a is transmitted.

The decision feedback decoding algorithm uses an estimate of the ML state at each RS state during the decoding. This estimate is updated after the survivor is found. Assume that these estimates for the current trellis section are as given in Fig. 9. These ML state estimates are

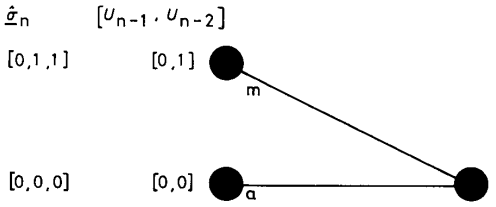

Fig. 9 *Paths used during decoding at RS state [0, 0] when ML state estimates are correct*

correct, meaning that no previous errors have occurred in the survivors or any previous errors do not any longer affect the decoding. Instead of selecting the best out of transitions a and i and e and m by a hard decision, the decoder use metrics based on the ML state estimates. These metrics are obtained in the same manner as for the ML VD for CPM, i.e. from the matched filters corresponding to transitions a and m. These two metric increments are added to the respective metrics of the survivors up to RS states [0, 0] and [0, 1] and the transition corresponding to the best metric is chosen as the survivor to RS state [0, 0], exactly as in the ML VD. The decoder uses a ML metric during this part of the decoding.

Table 5: Fusion of ML states for various RS state definitions

RS state $[U_{n-1}, U_{n-2}, V'_n(4, 3)$	fused from ML states $[U_{n-1}, U_{n-2}, V_n]$
[0, 0, 0]	[0, 0, 0], [0, 0, 4]
[0, 0, 1]	[0, 0, 1], [0, 0, 5]
[0, 0, 2]	[0, 0, 2], [0, 0, 6]
[0, 0, 3]	[0, 0, 3], [0, 0, 7]
RS state $[U_{n-1}, U_{n-2}, V'_n(2, 3)]$	**fused from ML states** $[U_{n-1}, U_{n-2}, V_n]$
[0, 0, 0]	[0, 0, 0], [0, 0, 2], [0, 0, 4], [0, 0, 6]
[0, 0, 1]	[0, 0, 1], [0, 0, 3], [0, 0, 5], [0, 0, 7]
RS state $[U_{n-1}, U_{n-2}]$	**fused from ML states** $[U_{n-1}, U_{n-2}, V_n]$
[0, 0]	[0, 0, 0], [0, 0, 1], [0, 0, 2], [0, 0, 3], [0, 0, 4] [0, 0, 5], [0, 0, 6], [0, 0, 7]
RS state $[U_{n-1}, V'_n(4, 2)]$	**fused from ML states** $[U_{n-1}, U_{n-2}, V_n]$
[0, 0]	[0, 0, 0], [0, 0, 4], [0, 1, 7], [0, 1, 3]
[0, 1]	[0, 0, 1], [0, 0, 5], [0, 1, 0], [0, 1, 4]
[0, 2]	[0, 0, 2], [0, 0, 6], [0, 1, 1], [0, 1, 5]
[0, 3]	[0, 0, 3], [0, 0, 7], [0, 1, 2], [0, 1, 6]
RS state $[U_{n-1}, V'_n(2, 2)]$	**fused from ML states** $[U_{n-1}, U_{n-2}, V_n]$
[0, 0, 0]	[0, 0, 0], [0, 0, 2], [0, 0, 4], [0, 0, 6], [0, 1, 7], [0, 1, 1], [0, 1, 3], [0, 1, 5]
[0, 0, 1]	[0, 0, 1], [0, 0, 3], [0, 0, 5], [0, 0, 7], [0, 1, 0], [0, 1, 2], [0, 1, 4], [0, 1, 6]

Assuming transition a leads to the best metric, this path is chosen as the survivor to RS state [0, 0]. The ML state estimate must be updated for RS state [0, 0]. This is done by using the information contained in the ML trellis. From the ML trellis it is clear that transition a from ML state [0, 0, 0], which is the ML state estimate at the origin RS state of transition a, ends in ML state [0, 0, 0], which is taken as the new ML state estimate at RS state [0, 0]. The algorithm then continues to the next RS state and repeats the same steps.

Assume that the ML state estimates are as shown in Fig. 10. Transition a is disregarded because of the erroneous ML state estimate at RS state [0, 0]. These two transitions do not enter the same state in the ML trellis. This demonstrates the effect of errors in the decision feedback decoder. The metric increments are obtained from the matched filters corresponding to transitions m and i. This means that the decoder use a mismatched metric, since the correct metric from the filter matched to transition a is not used during the decoding. This will degrade the performance, but as long as this does not cause error propagation it is not very harmful.

Assume that transition m gives the best metric. This means that this path is chosen as the survivor to RS state [0, 0]. The new ML state estimate at RS state [0, 0] is again found from the ML trellis and is given by [0, 0, 0]

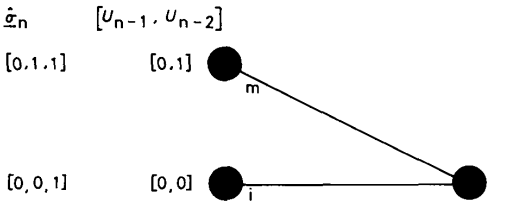

Fig. 10 *Paths used during decoding at RS state [0, 0] when ML state estimates are not correct*

which is the correct ML state estimate. This estimate is again correct in the next trellis section. This shows how the decision feedback decoder handles erroneous ML estimates. No case where errors lead to problems with error propagation has been found.